nature cell biology

Enhancing nucleotide metabolism protects against mitochondrial dysfunction and neurodegeneration in a *PINK1* model of Parkinson's disease

Roberta Tufi[1], Sonia Gandhi[2], Inês P. de Castro[1], Susann Lehmann[1], Plamena R. Angelova[2], David Dinsdale[1], Emma Deas[2], Hélène Plun-Favreau[2], Pierluigi Nicotera[3], Andrey Y. Abramov[2], Anne E. Willis[1], Giovanna R. Mallucci[1], Samantha H. Y. Loh[1,4] and L. Miguel Martins[1,4]

Mutations in *PINK1* cause early-onset Parkinson's disease (PD). Studies in *Drosophila melanogaster* have highlighted mitochondrial dysfunction on loss of Pink1 as a central mechanism of PD pathogenesis. Here we show that global analysis of transcriptional changes in *Drosophila pink1* mutants reveals an upregulation of genes involved in nucleotide metabolism, critical for neuronal mitochondrial DNA synthesis. These key transcriptional changes were also detected in brains of PD patients harbouring *PINK1* mutations. We demonstrate that genetic enhancement of the nucleotide salvage pathway in neurons of *pink1* mutant flies rescues mitochondrial impairment. In addition, pharmacological approaches enhancing nucleotide pools reduce mitochondrial dysfunction caused by Pink1 deficiency. We conclude that loss of Pink1 evokes the activation of a previously unidentified metabolic reprogramming pathway to increase nucleotide pools and promote mitochondrial biogenesis. We propose that targeting strategies enhancing nucleotide synthesis pathways may reverse mitochondrial dysfunction and rescue neurodegeneration in PD and, potentially, other diseases linked to mitochondrial impairment.

The role of mitochondrial impairment in PD has long been debated. Recently, the identification of causative mutations in *PINK1*, a gene encoding a mitochondrial kinase in PD patients has renewed interest in the role of mitochondrial damage in PD (ref. 1).

Cells have evolved several lines of defence to cope with damaged mitochondria[2]. Molecular quality control represents the first level of the mitochondrial defence mechanism. This involves the upregulation of nuclear genes that encode for mitochondrial chaperones and proteases that remove misfolded and non-assembled polypeptides in mitochondria, a form of mitochondrial retrograde signalling that is commonly referred to as the mitochondrial unfolded protein response[3] (UPR^{mt}).

Invertebrates such as *Drosophila* have recently emerged as powerful model systems to study the mechanisms of PD-associated neurodegeneration. These models are also excellent *in vivo* systems for the testing of therapeutic compounds[4].

Previously, we observed that *Drosophila pink1* mutants exhibit significant upregulation of key markers of the UPR^{mt} (ref. 5). To extend these observations, here we proceeded with an unbiased identification of upregulated transcripts in *pink1* mutant flies.

By combining transcriptional and metabolic profiling, we have uncovered significant alterations in the nucleotide metabolism networks of *pink1* mutant flies. In the cell, two metabolic pathways, referred to as the *de novo* and salvage pathways, are involved in nucleotide metabolism. Postmitotic cells such as neurons are reported to lack the *de novo* biosynthetic pathways for nucleotide generation and instead rely on the salvage pathway[6]. The conversion of deoxyribonucleosides (dNs) to their monophosphate forms is the rate-limiting step in the salvage pathway[7], and is catalysed by deoxyribonucleoside kinases (dNKs). *Drosophila dNK* is a highly efficient and multi-substrate single dNK acting on the nucleotide salvage pathway[8]. Here we show that both the genetic enhancement of the nucleotide salvage pathway by overexpression of *dNK* and the pharmacological manipulation of nucleotide metabolism enhance mitochondrial biogenesis, thus suppressing mitochondrial dysfunction associated with the PD phenotypes due to Pink1 deficiency.

Enhancement of nucleotide metabolism might therefore be of therapeutic benefit in human age-related neurological disorders linked to mitochondrial dysfunction.

[1]MRC Toxicology Unit, Lancaster Road, Leicester LE1 9HN, UK. [2]Department of Molecular Neuroscience, Institute of Neurology, Queen Square, London WC1N 3BG, UK. [3]German Centre for Neurodegenerative Diseases (DZNE), Ludwig-Erhard-Allee 2, 53175 Bonn, Germany.
[4]Correspondence should be addressed to S.H.Y.L. or L.M.M. (e-mail: shyl1@le.ac.uk or martins.lmiguel@gmail.com)

Received 3 April 2013; accepted 29 November 2013; published online 19 January 2014; DOI: 10.1038/ncb2901

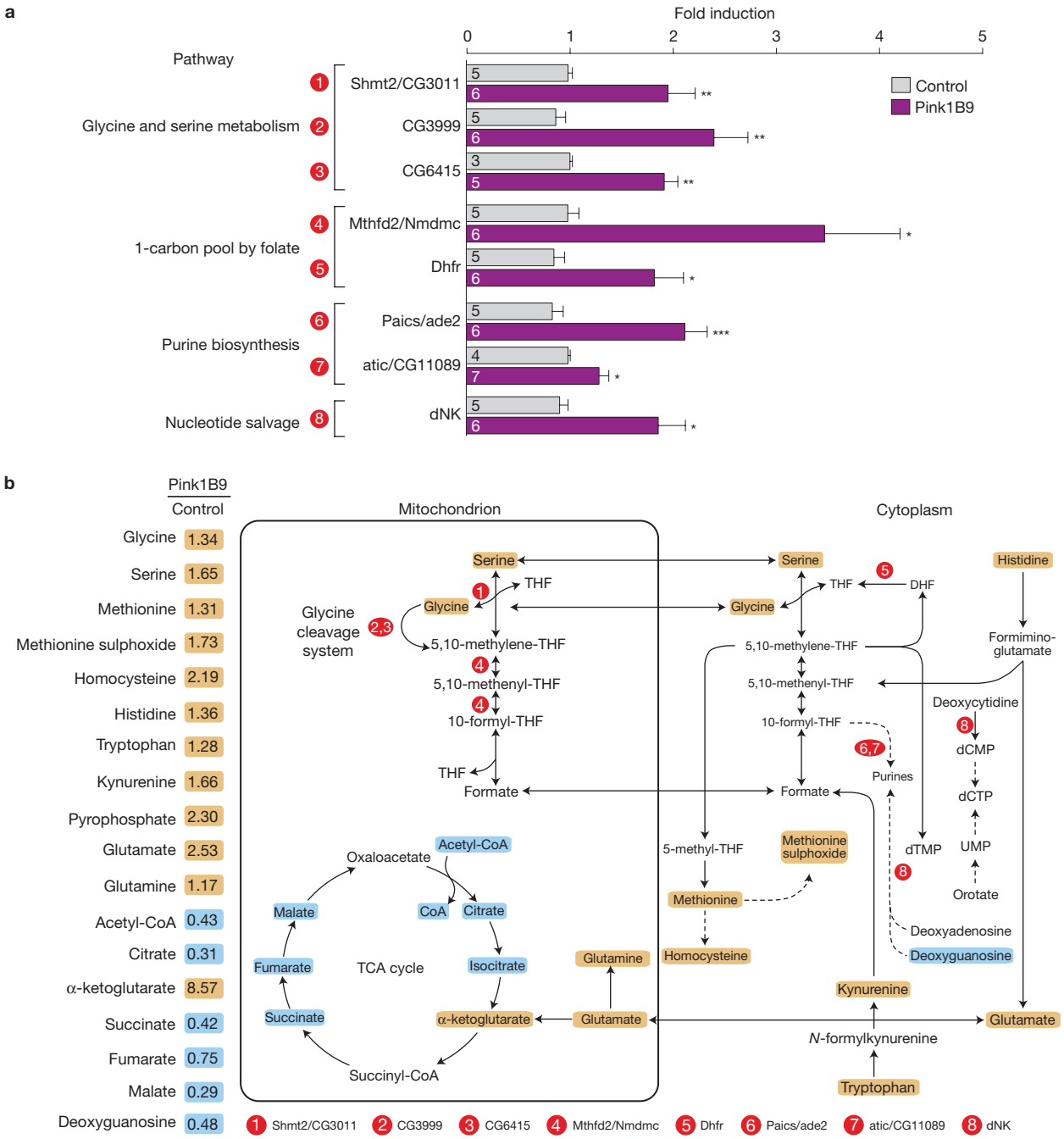

Figure 1 Loss of Pink1 results in a metabolic stress response. RNA and metabolites were isolated from 3-day-old control and *pink1* mutant male flies. (**a**) Quantitative validation by PCR with reverse transcription for a subset of genes found to be upregulated in the microarray analysis of *Drosophila pink1* mutants and that encode for metabolic enzymes. Circled numbers are related to the metabolic reactions shown in **b**. Data are shown as the mean ± s.e.m.; *n* values are indicated in the bars; asterisks, two-tailed unpaired *t*-test. See also Supplementary Fig. 1 and Tables 1–3 and 9 for statistics source data. (**b**) Coordinated changes in metabolite abundance on loss of *pink1* function. On the left, the relative levels of selected metabolites in *pink1* mutant flies, detected through gas chromatography with mass spectrometry and liquid chromatography with tandem mass spectrometry analysis. A schematic diagram is also shown, in which these metabolites are depicted with respect to the selected upregulated transcripts. Orange and cyan correspond to metabolites that are upregulated and downregulated, respectively, to a significant level. The statistical significance was determined using Welch's two-sample *t*-test ($n = 8$). See also Supplementary Fig. 1 and Tables 4 and 5.

RESULTS

Identification of an altered metabolic signature in *pink1* mutant flies

Previous studies have demonstrated that *Drosophila pink1* mutants exhibit transcriptional upregulation of the nuclear-encoded mitochondrial chaperones *hsp-60* and *hsc-70-5*, markers of the UPR^{mt} activation[5]. To determine the full complement of transcripts that are upregulated in *pink1* mutant flies, we employed microarray technology coupled with an *in silico* analysis approach (experimental outline, Supplementary Fig. 1a) . Using the RankProducts method to identify

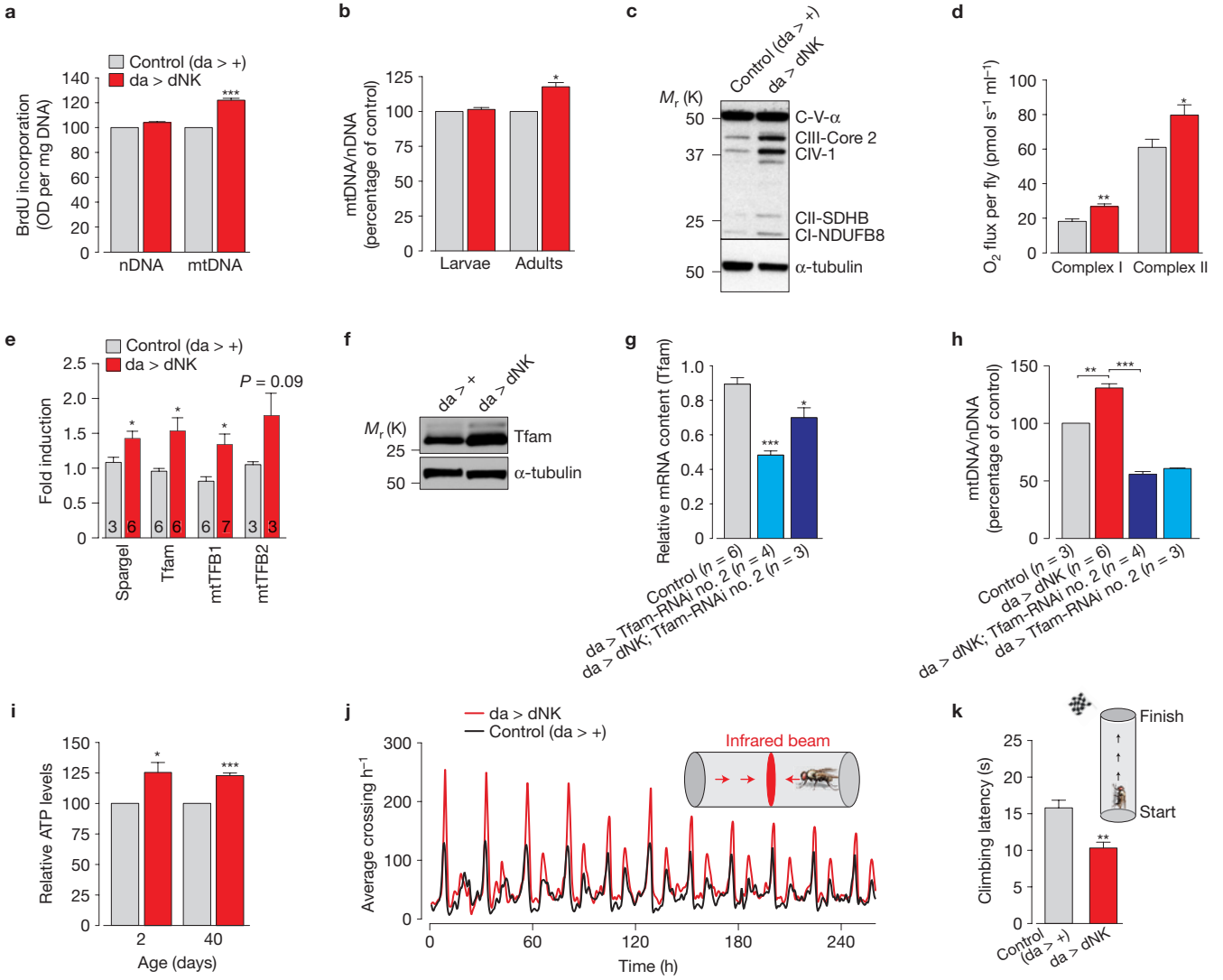

Figure 2 dNK enhances mitochondrial function by promoting organellar biogenesis. (**a**) Enhanced mtDNA synthesis in *dNK* transgenic flies. DNA synthesis was assessed using a BrdU assay (mean ± s.e.m.; $n = 12$; asterisks, two-tailed paired *t*-test). (**b**) *dNK* flies show an increase in mtDNA. The ratio of mtDNA to nuclear DNA (nDNA) was measured by real-time PCR using third-instar larvae and 2-day-old flies with the indicated genotypes (mean ± s.d.; $n = 9$; asterisks, two-tailed paired *t*-test). (**c**) *dNK* flies show an increase in mitochondrial oxidative phosphorylation proteins. Immunoblot of samples prepared from whole 2-day-old males. α-tubulin, loading control. (**d**) Enhanced respiration in *dNK* flies. Data are shown as the mean ± s.d. ($n = 3$ per genotype; asterisks, two-tailed unpaired *t*-test). (**e**) *dNK* flies show a transcriptional upregulation of the *PGC-1* family homologue *Spargel* and the nuclear-encoded mtDNA binding proteins Tfam, mtTFB1 and mtTFB2. Data are shown as the mean ± s.e.m. (*n* values are indicated in the bars; asterisks, two-tailed unpaired *t*-test). (**f**) dNK expression increases protein levels of mtTFA. Lysates prepared from adult flies were subjected to western blot analysis with the indicated antibodies. (**g**) RNAi-mediated suppression of *Tfam*. Expression levels were measured by real-time PCR (relative mean Ct ± s.e.m., *n* values are indicated). Statistically significant values relative to the control are indicated (one-way analysis of variance (ANOVA) with Bonferroni's multiple comparison test). (**h**) Tfam is required for the dNK-mediated increase in mtDNA. The ratio of mtDNA to nDNA was measured by real-time PCR using 2-day-old flies with the indicated genotypes (mean ± s.e.m.; *n* values are indicated; asterisks, one-way ANOVA with Bonferroni's multiple comparison test, $^{***}P < 0.0001$). (**i**) *dNK* expression results in a generalized ATP increase in both young (2-day-old) and old (40-day-old) flies. Data are shown as the mean ± s.d. from three independent experiments ($n = 3$ per genotype; asterisks, two-tailed paired *t*-test). (**j**) Ubiquitous expression of *dNK* enhances locomotor activity. Sixteen flies were tested for each genotype. (**k**) Ubiquitous expression of *dNK* enhances climbing ability. Flies were tested using a standard climbing assay (mean ± s.e.m.; $n = 100$ flies per genotype; asterisks, two-tailed unpaired *t*-test). See also Supplementary Figs 2 and 9 and Table 9 for statistics source data of **d**,**e**,**g**–**i**.

differentially expressed genes[9] and by selecting a relaxed false discovery rate of 50%, we detected a large number of upregulated transcripts in *pink1* mutants (Supplementary Table 1). We next employed iterative Group Analysis[10] to identify functional classes of genes that were significantly upregulated in mutant flies (Supplementary Fig. 1b and Table 2). This approach confirmed the upregulation of stress-related genes that code for chaperones previously detected in *pink1* mutants[5]. Interestingly, we also identified the upregulation of components of the glycine cleavage system, a mitochondrial enzymatic complex involved in glycine catabolism[11], and the upregulation of genes that belong to the purine biosynthetic pathway. Glycine catabolism is directly related to purine biosynthesis because glycine provides the C4, C5 and N7 atoms

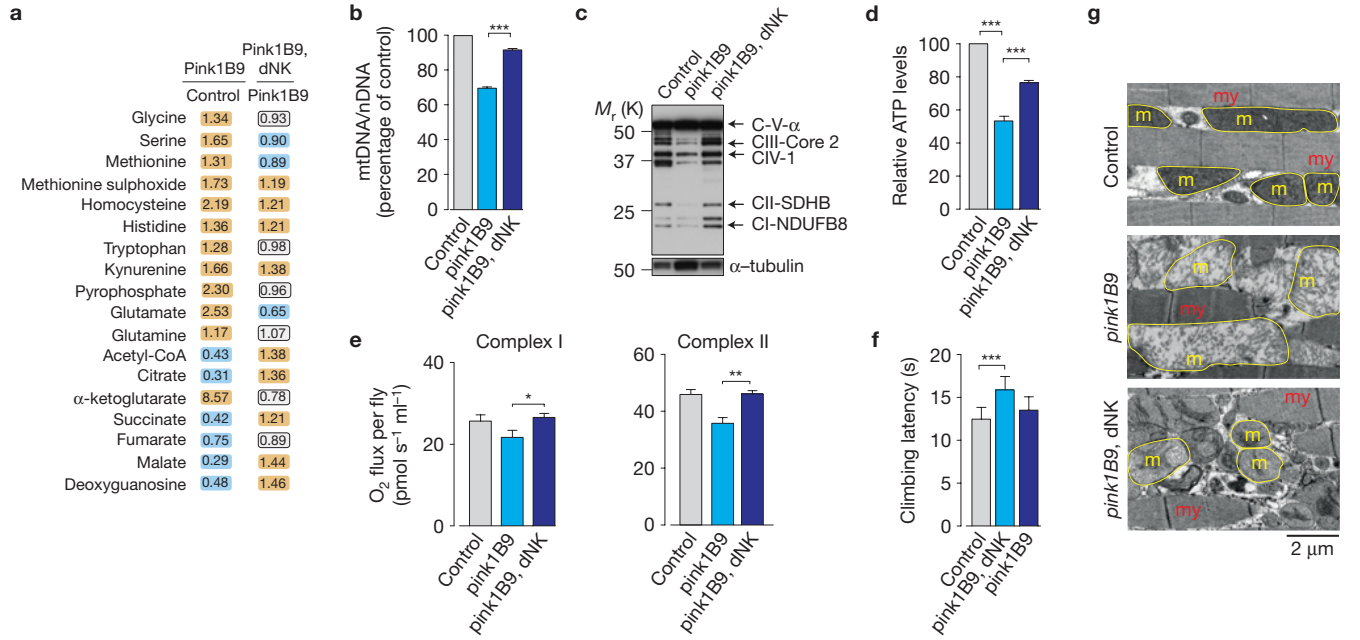

Figure 3 Mitochondrial dysfunction in *Drosophila pink1* mutants is complemented by *dNK*. (**a**) Expression of *dNK* partially reverses metabolic shifts in *pink1* mutants. Orange and cyan correspond to metabolites that are upregulated and downregulated, respectively, to a significant level. The statistical significance was determined using Welch's two-sample *t*-test ($n=8$). See also Supplementary Table 6. (**b**) *dNK* expression increases mtDNA levels in *pink1* mutants. The ratio of mtDNA to nDNA was measured by real-time PCR in flies with the indicated genotypes (mean ± s.d.; $n=6$ per genotype; asterisks, one-way ANOVA with Bonferroni's multiple comparison test). (**c**) Expression of *dNK* restores the levels of mitochondrial respiratory complexes in *pink1* mutants. Whole-fly lysates were analysed by western blot analysis using the indicated antibodies. (**d**) *dNK* expression rescues ATP levels in *pink1* mutants. Data are shown as the mean ± s.d. ($n=6$ per genotype; asterisks, one-way ANOVA with Bonferroni's multiple comparison test). (**e**) *dNK* expression enhances respiration in *pink1* mutants. Data are shown as the mean ± s.d. ($n=3$ per genotype; asterisks, two-tailed unpaired *t*-test). See Supplementary Table 9 for statistics source data. (**f**) *dNK* expression suppresses motor impairment in *pink1* mutants. Flies were tested using a standard climbing assay (mean ± s.e.m.; $n=100$ flies per genotype; asterisks, one-way ANOVA with Dunnett's multiple comparison test). (**g**) *dNK* expression suppresses flight muscle defects observed in *pink1* mutants. *dNK* expression rescues mitochondrial defects in *pink1* mutants (my, myofibrils; m, mitochondria; yellow outlines, mitochondria). See also Supplementary Figs 3 and 9.

to the purine ring. Next, through network analysis, we uncovered an enrichment for components involved in glycine catabolism and folate metabolism in *pink1* mutant flies (Supplementary Fig. 1c and Tables 3 and 4). This combined approach identified groups and networks of genes that were positively regulated in *pink1* mutants and belong to metabolic pathways related to nucleotide biosynthesis. We then sought to confirm the upregulation of components of both the *de novo* and salvage nucleotide synthesis pathways in *pink1* mutant flies. We detected a significant increase in components of the *de novo* nucleotide biosynthesis pathway, related to glycine, serine and folate metabolism. Importantly, we also confirmed the upregulation of *dNK*, a master regulator of the salvage pathway of nucleotide synthesis (Fig. 1a).

To investigate whether the observed upregulation of these genes reflects an altered metabolic state, we analysed the global metabolic changes in *pink1* mutants. This revealed that approximately 60% of the measured biochemicals are significantly altered in *pink1* mutants (Fig. 1b and Supplementary Table 5). We observed a clear decrease in most tricarboxylic acid (TCA) cycle metabolites and increases in α-ketoglutarate, glutamate and glutamine. Glutamate can be converted to α-ketoglutarate through glutaminolysis, thereby compensating for losses of the TCA cycle (reviewed in ref. 12). In addition, glutamine is an important source of nitrogen for purine and pyrimidine synthesis.

This analysis also revealed significant increases in metabolites that are associated with nucleotide catabolism, such as nucleoside cytidine, and salvage, such as pyrophosphate. These data led us to reason that on mitochondrial dysfunction caused by the loss of Pink1 activity, cells attempt to enhance the nucleotide pool to compensate for mitochondrial impairment.

dNK enhances mitochondrial function by promoting organellar biogenesis

To test the hypothesis that the enhancement of nucleotide pools is a compensatory mechanism following mitochondrial dysfunction, we decided to manipulate the expression of *dNK*, the rate-limiting enzyme in the nucleotide salvage pathway. *dNK* expression is upregulated in *pink1* mutants (Fig. 1a and Supplementary Table 1) and enhanced expression of *dNK* is associated with mitochondrial biogenesis[13].

We first noted that the ubiquitous expression of *dNK* led to a specific increase in mitochondrial DNA (mtDNA; Fig. 2a,b), accompanied by an increase in mitochondrial proteins (Fig. 2c), suggesting that *dNK* expression increased mitochondrial mass in flies. This also resulted in a significant increase in the oxygen consumption (Fig. 2d and Supplementary Fig. 2a).

Mitochondrial biogenesis is achieved by the coordinated regulation of different gene subsets by the PPARγ coactivator −1α (PGC-1α) that promotes the nuclear respiratory factor 1 (NRF-1)-dependent transcriptional upregulation of nuclear-encoded mitochondrial proteins. We found that *dNK* promotes an increase in the messenger

RNA levels of both *Spargel*, the orthologue of the *PGC-1* family, and the nuclear-encoded mitochondrial proteins Tfam, mtTFB1 and mtTFB2 (Fig. 2e). After confirming the upregulation of the Tfam protein levels (Fig. 2f), we decided to test the effects of its loss for the dNK-dependent mtDNA increase by downregulating *Tfam* expression using RNA interference (Fig. 2g). *Tfam* knockdown (KD) alone resulted in mtDNA depletion (Tfam-RNAi no. 2 line) and, in *dNK*-expressing flies, it abolished the dNK-induced mtDNA increase (Fig. 2h), indicating a requirement for Tfam in the dNK-dependent induction of mitochondrial biogenesis.

This biogenesis was reflected in elevated ATP levels (Fig. 2i) and in the generalized increase in the locomotor activity of flies expressing *dNK* (Fig. 2j,k and Supplementary Fig. 2b). *dNK*-expressing flies have a modest decrease in lifespan (Supplementary Fig. 2c) but an increase in survival when challenged with mitochondrial poisons (Supplementary Fig. 2d,e), and this is also associated with enhanced levels of mitochondrial reactive oxygen species detoxification components such as the superoxide dismutases 1 and 2 (SOD1 and SOD2; Supplementary Fig. 2f).

Expression of *dNK* rescues mitochondrial dysfunction in *pink1* mutant flies

We next examined the effects of inducing mitochondrial biogenesis in *pink1* mutants by overexpressing *dNK*. Global metabolic analysis revealed that dNK promoted increases in the levels of glucose, glucose-6-phosphate (G6P) and the TCA cycle intermediates (Fig. 3a and Supplementary Table 6), indicating that *dNK* expression induced a partial recovery of mitochondrial metabolism. We also observed an increase in the level of the dNK substrate deoxyguanosine. Further analysis revealed that *dNK* expression rescued the loss of mtDNA (Fig. 3b), mitochondrial proteins (Fig. 3c and Supplementary Fig. 3a) and ATP (Fig. 3d) and reversed the respiration defects (Fig. 3e and Supplementary Fig. 3b) of *pink1* mutants. *dNK* expression also resulted in the significant suppression of motor impairment in *pink1* mutants (Fig. 3f), recovery of mitochondrial cristae fragmentation defects in the indirect flight muscle (Fig. 3g and Supplementary Fig. 3c), significant reduction of crushed thorax defects (Supplementary Fig. 3d,e) and increased resistance to antimycin toxicity (Supplementary Fig. 3f). In flies, the absence of Pink1 results in defective mitophagy linked to the accumulation of dMfn in damaged mitochondria[14]. The expression of *dNK* had no effects on the levels of dMfn in either control or *pink1* mutant flies, suggesting that the dNK-dependent increase in mitochondrial mass is not linked to defects in the removal of defective mitochondria through mitophagy (Supplementary Fig. 3g). These data suggest that ubiquitous dNK-mediated enhancement of the nucleotide salvage pathway promotes mitochondrial biogenesis and this rescues mitochondrial dysfunction in *pink1* mutants.

Neuronal expression of *dNK* reverts the phenotype of *pink1* mutants

In *Drosophila* neurons, Pink1 deficiency leads to defects in synaptic transmission[15]. As one of the most prominent features of *pink1* mutant flies is the degeneration of the indirect flight muscle[16], we investigated whether this involves a presynaptic component. First, we confirmed the upregulation of components of both the *de novo* and salvage nucleotide synthesis pathways in the heads of *pink1*

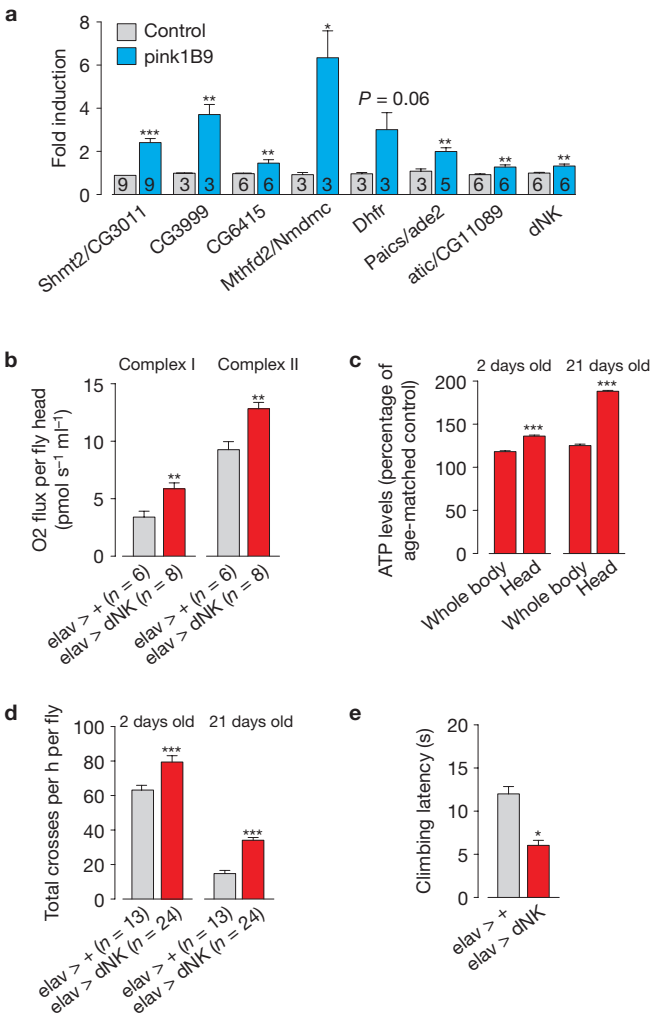

Figure 4 Targeted neuronal expression of *dNK* rescues mitochondrial dysfunction in *pink1* mutants. (**a**) Enhanced expression of components of both the *de novo* and salvage nucleotide synthesis pathways in adult heads of *pink1* mutant flies. Data are shown as the mean ± s.e.m. (*n* values are indicated in the bars; asterisks, two-tailed unpaired *t*-test). See Supplementary Table 9 for statistics source data. (**b**) Enhanced respiration in the heads of elav > dNK flies. Data are shown as the mean ± s.e.m. (*n* values are indicated; asterisks, two-tailed unpaired *t*-test). (**c**) Neuronal expression of *dNK* enhances ATP levels. Data are shown as the mean ± s.e.m. ($n = 6$ per sample; asterisks, two-tailed unpaired *t*-test). (**d**) Neuronal expression of *dNK* enhanced locomotor activity. Data are shown as the mean ± s.e.m. (*n* values are indicated; asterisks, two-tailed unpaired *t*-test). (**e**) Neuronal expression of *dNK* enhanced climbing ability (mean ± s.e.m.; $n = 100$ flies per genotype; asterisks, two-tailed unpaired *t*-test). See also Supplementary Fig. 4.

mutant flies (Fig. 4a). Next, we examined the effects of the neuronal expression of *dNK* in *pink1* mutant flies. The neuronal expression of *dNK* resulted in enhancements in the respiration and ATP levels (Fig. 4b,c), an increase in the total locomotor activity (Fig. 4d) and an improved climbing performance (Fig. 4e). *Drosophila pink1* mutants exhibit a loss of dopaminergic neurons[16], the extent of which can be assessed through analysis of the expression levels of tyrosine hydroxylase, an enzyme expressed in dopaminergic neurons[17]. We detected a decrease in the tyrosine hydroxylase levels in *pink1* mutants that was reversed on the neuronal expression of *dNK*

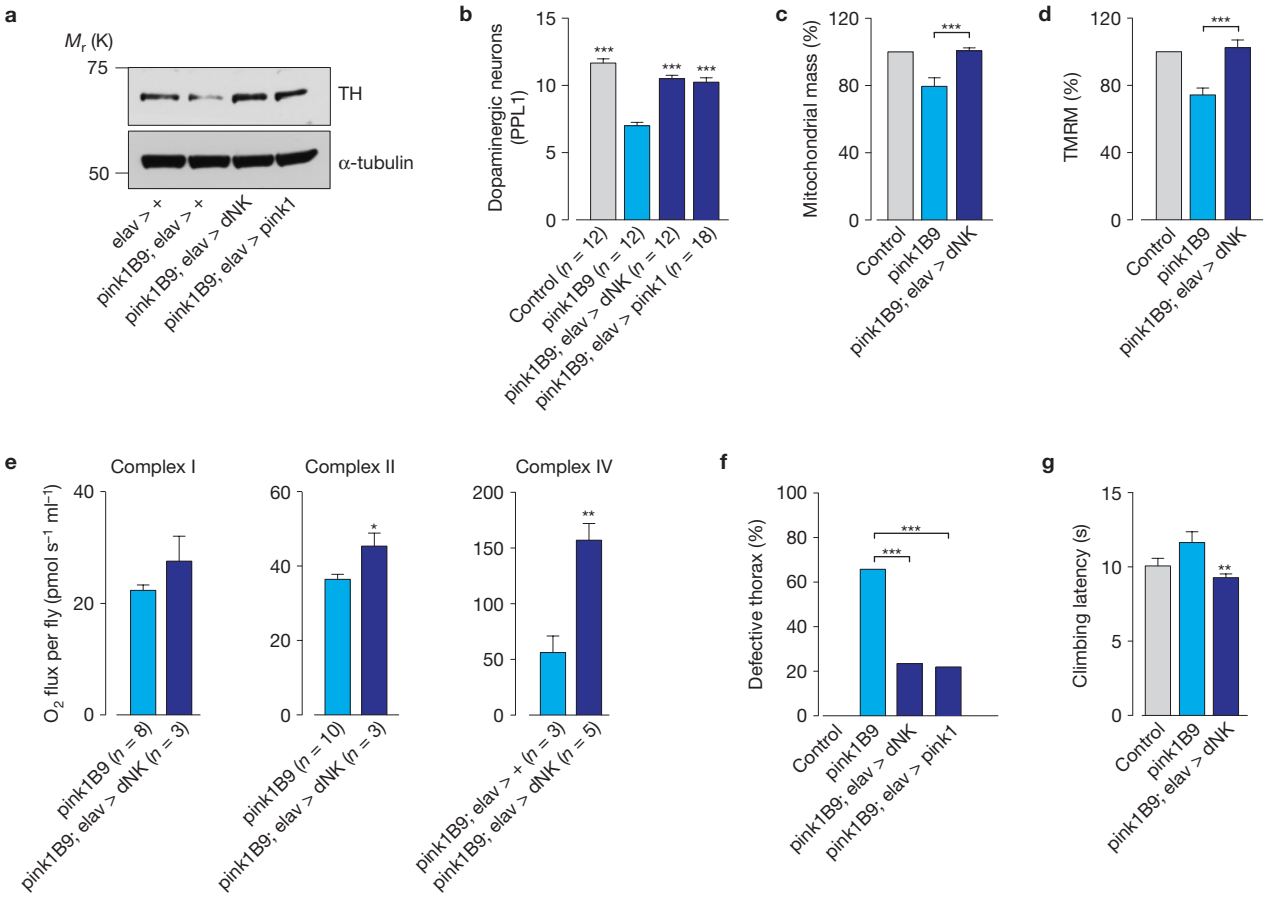

Figure 5 Targeted neuronal expression of *dNK* rescues neurodegeneration in *pink1* mutants. (**a**) Neuronal expression of *dNK* restores the tyrosine hydroxylase (TH) levels in *pink1* mutants. Fly head lysates were analysed using the indicated antibodies. (**b**) Expression of *dNK* rescues the loss of dopaminergic neurons in the PPL1 cluster of *pink1* mutant flies. Data are shown as the mean ± s.e.m. (*n* values are indicated; asterisks, one-way ANOVA with Bonferroni's multiple comparison test). Data sets labelled control and pink1B9 are also used in Fig. 6h,i. (**c**) Neuronal expression of *dNK* promotes an increase in neuronal mitochondrial mass of *pink1* mutants. Mitochondrial mass was calculated as the ratio of co-localization between the TMRM signal (mitochondria) and calcein blue (whole cells). Data are the mean ± s.e.m. ($n = 6$ per genotype; asterisks, two-tailed paired *t*-test). Data sets labelled control and pink1B9 are also used in Fig. 6d,e. (**d**) Neuronal expression of *dNK* reverses the loss of Δψm in *pink1* mutants. The Δψm is represented as percentage of control. Data are shown as the mean ± s.e.m. ($n = 7$ per genotype; asterisks, two-tailed unpaired *t*-test). Data sets labelled control and pink1B9 are also used in Fig. 6f,g. (**e**) Neuronal expression of *dNK* enhances respiration in *pink1* mutants. Data are shown as the mean ± s.d. (*n* values are indicated, asterisks; two-tailed unpaired *t*-test). Complex I and II, and complex IV were measured in coupled and uncoupled mitochondria, respectively. See Supplementary Table 9 for statistics source data. (**f**) Neuronal expression of *dNK* rescues the thoracic defects of *pink1* mutants ($n = 255$ for pink1B9, $n = 227$ for pink1B9; elav > dNK, $n = 187$ for pink1B9; elav > pink1); asterisks, χ^2 two-tailed, 95% confidence intervals). (**g**) Neuronal expression of *dNK* rescues the motor impairment of *pink1* mutants. Mean ± s.e.m.; $n = 100$ flies per genotype; asterisks, two-tailed paired *t*-test, relative to pink1B9). See also Supplementary Figs 5 and 9.

(Fig. 5a). Accordingly, the neuronal expression of *dNK* rescued the dopaminergic neuron loss in the protocerebral posterior lateral 1 (PPL1) cluster of *pink1* mutants (Fig. 5b). To determine whether dNK-dependent suppression of neurodegeneration in *pink1* mutants was linked to a neuronal rescue of mitochondrial function, we assessed mitochondrial mass and potential (Δψm) in fly brains (Supplementary Fig. 4a). We detected a decrease of both mitochondrial mass and Δψm in *pink1* mutants that was reversed on neuronal expression of *dNK* (Fig. 5c,d).

The neuronal expression of *dNK* was also sufficient to promote the recovery of defects in respiration (Fig. 5e) and ATP levels (Supplementary Fig. 4b) in *pink1* mutants. Notably, the neuronal expression of *dNK* in *pink1* mutants significantly decreased the presence of the crushed thorax phenotype (Fig. 5f), improved climbing performance (Fig. 5g) and suppressed flight defects (Supplementary Fig. 4c). In addition, neuronal expression of *pink1* was sufficient to suppress mitochondrial cristae fragmentation defects in the indirect flight muscle of *pink1* mutants (Supplementary Fig. 4d). These effects indicate that the neuronal rescue of mitochondrial function in *pink1* mutants is sufficient to suppress indirect flight muscle degeneration and motor impairment. Parkin acts as a downstream effector of PINK1 as highlighted in a series of studies in *Drosophila*, which demonstrated that the expression of *parkin* rescues the phenotype of *pink1* mutant flies[16,18]. To test the epistatic relationship between *parkin* and *dNK*, we determined whether the neuronal expression of *dNK* could also rescue the phenotype of *parkin* mutants. We detected a decrease of Δψm in *parkin* mutants that was reversed on neuronal expression of *dNK* (Supplementary Fig. 5a). In addition, the neuronal expression of *dNK* was sufficient to rescue the neurodegeneration (Supplementary Fig. 5b), the presence of the crushed thorax phenotype (Supplementary Fig. 5c)

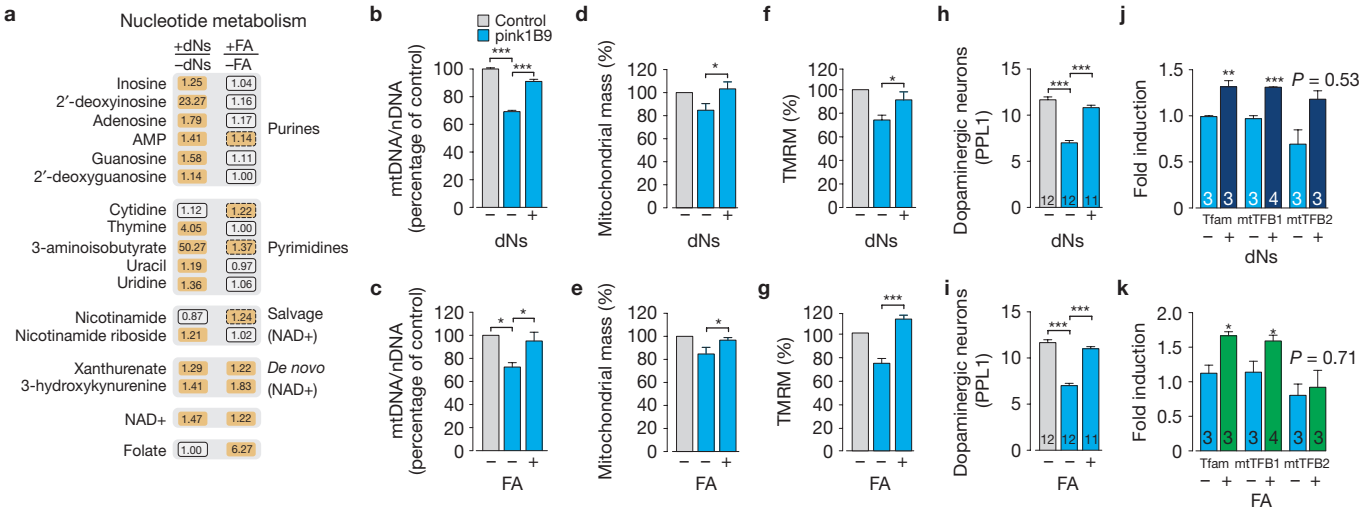

Figure 6 Dietary supplementation with dNs or FA enhances mitochondrial function and biogenesis in *pink1* mutants. (**a**) Dietary supplementation with dNs (0.5 mg ml^{-1} each dN) or FA (4 mM) promotes an upregulation of biochemical components of nucleotide metabolism pathways in *pink1* mutants. Orange corresponds to metabolites that are upregulated to a significant level ($P < 0.05$). Orange oblongs with a dashed outline correspond to comparisons with lower statistical significance ($0.05 < P < 0.10$). Statistical significance was determined using Welch's two-sample *t*-test ($n = 5$). See also Supplementary Table 7. (**b**,**c**) Dietary supplementation with dNs (**b**) or FA (**c**) during the adult stage promotes an increase in mtDNA. The ratio of mtDNA to nDNA was measured by real-time PCR using 2-day-old flies with the indicated genotypes (mean ± s.d. $n = 9$ (**b**), $n = 3$ (**c**) per genotype). Statistically significant values are indicated by asterisks (one-way ANOVA with Bonferroni's multiple comparison test). (**d**,**e**) dNs or FA promote an increase in neuronal mitochondrial mass of *pink1* mutants. Data are shown as the mean ± s.e.m. ($n = 6$ for dNs, $n = 7$ for FA). Statistical significance is indicated by asterisks (two-tailed paired *t*-test). Data sets labelled control and pink1B9 are also used in Fig. 5c (**f**,**g**) dNs or FA reverse the loss of $\Delta\psi$m in *pink1* mutants. The $\Delta\psi$m is represented as percentage of control. The error bars represent the mean ± s.e.m. ($n = 7$). Statistical significance is indicated by asterisks (two-tailed unpaired *t*-test). Data sets labelled control and pink1B9 are also used in Fig. 5d. (**h**,**i**) dNs or FA reverse the loss of dopaminergic neurons in the PPL1 cluster of *pink1* mutants. Data are shown as the mean ± s.e.m. (*n* values are indicated in the bars; asterisks, one-way ANOVA with Bonferroni's multiple comparison test). Data sets labelled control and pink1B9 are also used in Fig. 5b. (**j**,**k**) dNs or FA promote the transcriptional upregulation of the nuclear-encoded mtDNA-binding proteins Tfam, mtTFB1 and mtTFB2 in *pink1* mutants. The error bars represent s.e.m. values (*n* values are indicated in the bars), and the asterisks indicate statistically significant values (two-tailed unpaired *t*-test) relative to *pink1* flies on a normal diet. See also Supplementary Fig. 6 and Table 9 for statistics source data of **c**,**j** and **k**.

and the degree of mitochondrial cristae fragmentation defects in the indirect flight muscle (Supplementary Fig. 5d) of *parkin* mutants.

dNs and folate stimulate mitochondrial biogenesis and suppress mitochondrial dysfunction in *pink1* mutant flies

Our findings show that in the context of reduced dNK substrate availability (Fig. 1b), *pink1* mutant flies attempt to compensate for mitochondrial stress by inducing the expression of *dNK*. To investigate the effects of enhancing the availability of dNK substrates in *pink1* mutants, we exposed the mutants to a diet supplemented with a mixture of the four main dNs: deoxyadenosine, deoxythymidine, deoxycytidine and deoxyguanosine. We found significant changes in approximately 37% of the biochemicals detected in mutant flies raised on food supplemented with all four dNs (Supplementary Table 7). Dietary dNs promoted increases in the dNK substrate 2′-deoxyguanosine, 2′-deoxyinosine and thymine, and led to an increase in biochemical intermediates of nucleotide metabolism (Supplementary Table 7 and Fig. 6a).

On loss of Pink1, flies respond by transcriptional upregulation of genes of the *de novo* pathway of nucleotide biosynthesis. As a result of the addition of 1-carbon units in this pathway, folic acid (FA) plays a fundamental role in nucleotide synthesis. Therefore, we reasoned that administering FA to *pink1* mutants could promote nucleotide biosynthesis and confer a protective effect on mitochondria. First, we analysed the metabolic response to feeding mutant flies with FA, and found that a FA-supplemented diet led to changes in approximately 18% of the biochemicals detected (Supplementary Table 7). As with dNs, we detected increases in biochemical intermediates of NAD+ synthesis, as well as more subtle increases in components of purine and pyrimidine biosynthesis (Supplementary Table 7 and Fig. 6a). Taken together, these changes suggest that in the absence of Pink1, supplementation with dNs or FA leads to increases in nucleotide metabolism, in particular in the NAD+ *de novo* and salvage pathways, with a resulting increase in the NAD+ pools.

We next examined the ability of dNs and FA to suppress mitochondrial dysfunction in *pink1* mutants. Administration of either dNs or FA to *pink1* mutant adults caused an increase in mtDNA (Fig. 6b,c), mitochondrial mass (Fig. 6d,e), potential (Fig. 6f,g) and ATP levels (Supplementary Fig. 6a). Moreover, dNs- or FA-supplemented diet rescued the dopaminergic neuron loss of *pink1* mutants (Fig. 6h,i). Importantly, we detected a transcriptional upregulation of Tfam, mtTFB1 and mtTFB2 (Fig. 6j,k). Again, neither dNs nor FA had an effect on the levels of dMfn (Supplementary Fig. 6b), suggesting that the main effects of these compounds in *pink1* mutants are linked to supporting mitochondrial biogenesis.

Maintaining *pink1* mutants on a dNs- or FA-supplemented diet significantly reduced the appearance of defective thorax phenotype (Fig. 7b), and suppressed mitochondrial cristae fragmentation defects (Fig. 7a and Supplementary Fig. 7a) and flight defects (Fig. 7c). Moreover, the sole provision of either dNs or FA to adult mutants

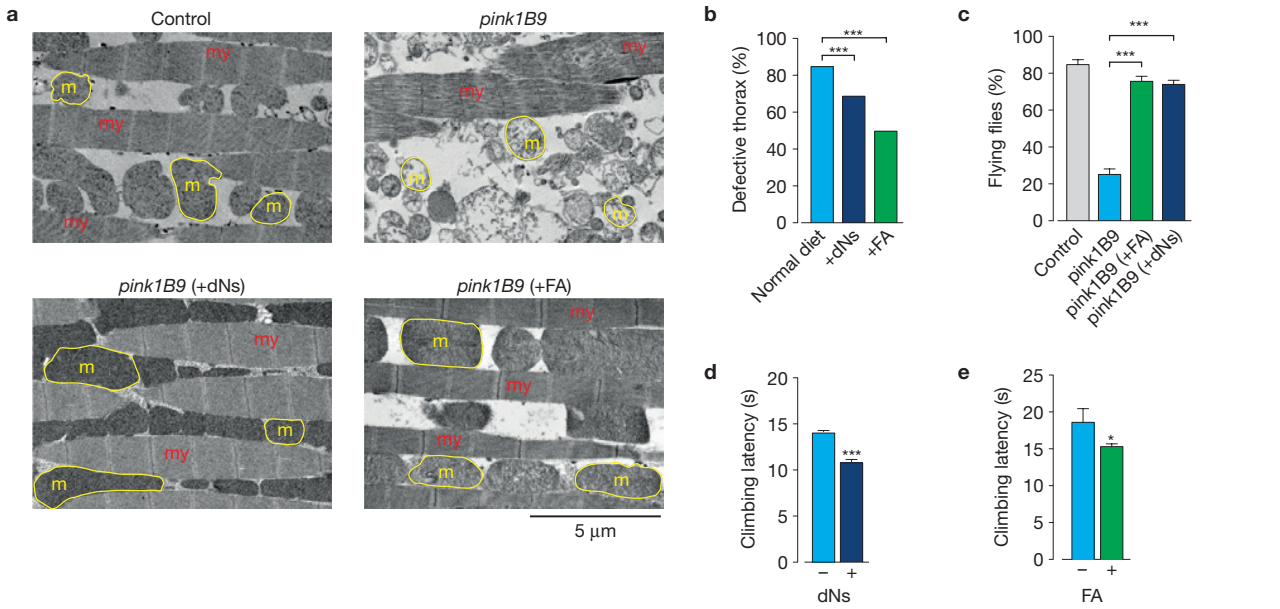

Figure 7 Dietary supplementation with dNs or FA suppresses *pink1* mutant phenotypes. (**a**) Suppression of flight muscle degeneration and mitochondrial defects in *pink1* mutants by dNs or FA. Ultrastructural analysis of the indirect flight muscles from *pink1* mutant flies raised on dNs- or FA-supplemented food (my, myofibrils; m, mitochondria; yellow outlines, mitochondria). (**b**) Dietary supplementation with dNs or FA rescues the thoracic defects of *pink1* mutants. *pink1* mutants were exposed to a dNs- or FA-supplemented diet after egg laying. *P* values are indicated by asterisks (χ^2 two-tailed, 95% confidence intervals, $n = 454$ for normal diet, $n = 448$ for +dNs and $n = 669$ for +FA). (**c**) Dietary supplementation with dNs or FA rescues the flight defects of *pink1* mutants. Data are shown as mean ± s.e.m. ($n = 150$ flies per condition). Statistically significant values relative to pink1B9 are indicated by asterisks (one-way ANOVA with Bonferroni's multiple comparison test). Data sets labelled control and pink1B9 are also used in Supplementary Fig. 4c. (**d**,**e**) Dietary supplementation with dNs or FA during adult stage rescues the motor impairment of *pink1* mutants. *pink1* mutants were exposed to a dNs- or FA-supplemented diet after eclosion. Flies were tested using a standard climbing assay (mean ± s.e.m., $n = 100$ flies per condition). Statistical significance is indicated (two-tailed unpaired *t*-test). See also Supplementary Fig. 7.

resulted in improved climbing performance (Fig. 7d,e). We also observed that purines were more efficient in the suppression of the crushed thorax phenotype in *pink1* mutants when compared with pyrimidines (Supplementary Fig. 7b). Next we investigated whether dNs or FA could also rescue the phenotype of *parkin* mutants. Maintaining *parkin* mutants on a dNs- or FA-supplemented diet rescued the loss of $\Delta\psi$m (Supplementary Fig. 7c) and dopaminergic neurons (Supplementary Fig. 7d), and the indirect flight muscle defects (Supplementary Fig. 7e,f). Together, these results suggest that both dNs- and FA-mediated enhancement of nucleotide pools and mitochondrial biogenesis compensate for the mitochondrial dysfunction observed on disruption of the Pink1–Parkin pathway.

dNs and folate restore mitochondrial functional impairment in *PINK1* KD human cells

To determine whether the transcriptional upregulation of genes involved in nucleotide metabolism observed in *pink1* mutant flies was present in PD patients carrying *PINK1* mutations, we analysed the expression of key genes in post-mortem brain tissue of patients with *PINK1* mutations. Samples were selected on the basis of RNA quality (Supplementary Fig. 8) and the expression levels of specific mRNAs were measured. We detected an increase in the mRNA levels of genes of the *de novo* purine biosynthesis pathway, in *DHFR* and in the mitochondrial thymidine kinase 2 (*TK2*), the closest orthologue of *Drosophila dNK* (Fig. 8a).

We next investigated whether the exogenous supply of either dNs or FA could modulate mitochondrial bioenergetics and function in PINK1 KD cells. Pre-incubation of PINK1 KD cells with either dNs (Fig. 8b(i)) or FA (Fig. 8b(ii)) led to a significant recovery in the tetramethylrhodamine, methyl ester (TMRM) signal, indicating that both treatments can rescue the loss of basal $\Delta\psi$m resulting from a deficiency of PINK1 in human cells.

As a result of complex V maintaining the $\Delta\psi$m in PINK1 KD cells[19], inhibition of complex V by oligomycin results in a rapid mitochondrial depolarization and a decrease in TMRM fluorescence (Fig. 8c(i)), which was reversed by dNs or FA (Fig. 8c). Incubation of cells with dNs or FA resulted in minimal depolarization of the mitochondrial membrane potential in response to oligomycin and rapid depolarization in response to complex I inhibition by rotenone (Fig. 8c(ii),c(iii)). These data suggest that dNs and FA are able to improve respiration sufficiently to maintain the mitochondrial membrane potential, and thus also enable complex V to function as an ATP synthase rather than an ATPase.

The redox state of the complex I substrate NADH is a function of both respiratory chain activity and the rate of substrate supply. Human PINK1 KD cells show a shift towards a more oxidized redox state[19]. To determine the effects of dNs and FA on the redox state of NADH, we measured the resting level of NADH autofluorescence and generated the 'redox index', a ratio of the maximally oxidized (response to 1 µM FCCP) and maximally reduced (response to 1 mM NaCN) signals. The exogenous supply of both dNs and FA restored the basal NADH level in PINK1 KD neuroblastoma cells to values equivalent to those in the controls (Fig. 8d,e).

Restoration of the NADH pool by dNs and FA would improve availability of NADH to complex 1, resulting in improved respiration

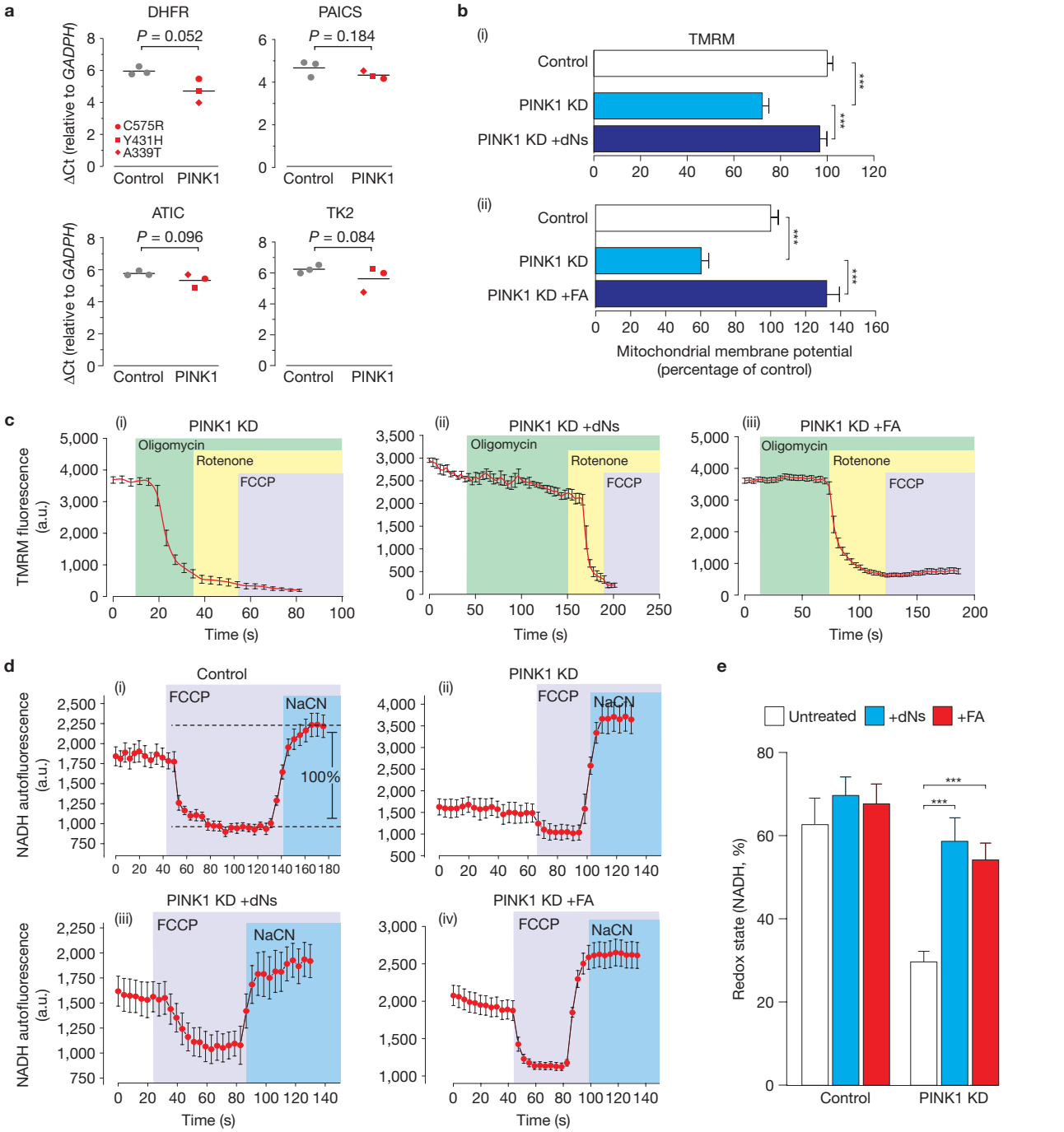

Figure 8 An exogenous supply of dNs and FA suppresses mitochondrial dysfunction on loss of *PINK1* in human neuroblastoma cells. (**a**) Genes encoding for enzymes of the purine biosynthetic and nucleotide salvage pathways are significantly upregulated in a subset of PD patients with *PINK1* mutations. Delta Ct values (ΔCt) for each of the analysed transcripts were normalized to *GAPDH*. Means are represented by horizontal bars. *P* values (two-tailed unpaired *t*-test) relative to controls are indicated. See Supplementary Table 9 for statistics source data. (**b**) An exogenous supply of dNs (i) or folate (ii) reversed the reduction in the basal mitochondrial membrane potential in *PINK1* KD cells. Cells were grown for 24 h in media supplemented with dNs (20 μM each dN) or FA (300 μM) and were compared with cells grown in normal media. (i) Mean ± s.e.m., $n = 240$ cells of three separate clones, data from 6 independent experiments. (ii) Mean ± s.e.m., $n = 180$ cells of three separate clones, data from 6 independent experiments. Statistical significance is indicated by asterisks (two-tailed paired *t*-test). (**c**) The reversal of oligomycin-induced $\Delta\psi m$ by dNs and FA. In *PINK1* KD cells (i), oligomycin caused marked mitochondrial depolarization, whereas the exogenous addition of either dNs (ii) or FA (iii) completely blocked depolarization. Cells were grown for 24 h in media supplemented with dNs (20 μM each dN) or FA (300 μM) and were compared with cells grown in normal media. Error bars represent mean ± s.e.m. ($n = 180$ cells). (**d**,**e**) Reversal of the loss of the NADH redox state in *PINK1* KD cells by dNs and FA. The resting level of NADH autofluorescence was measured by determining the ratio between the signal for the maximally oxidized condition (response to 1 μM FCCP) and the signal for the maximally reduced condition (response to 1 mM NaCN) to determine the baseline redox state in control cells (i). PINK1 KD cells showed a decreased redox state (**d**(ii) and **e**), whereas the exogenous supply of either dNs or FA recovered the redox state (**d**(iii), **d**(iv) and **e**). Cells were grown for 24 h in media supplemented with dNs (20 μM each dN) or FA (300 μM) and were compared with cells grown in normal media. The error bars represent the mean ± s.e.m. ($n = 180$ cells). Statistical significance is indicated by asterisks (two-tailed paired *t*-test).

and the switch to normal maintenance of the mitochondrial membrane potential by the ETC, and ATP synthesis by complex V.

DISCUSSION

Mitochondria operate a sensitive feedback system, the retrograde response, to adjust their performance[20]. This was originally discovered in yeast[21], and is a pathway of communication from mitochondria to the cell nucleus. We now show that there is an additional, previously uncharacterized, branch of the retrograde response that is activated on mitochondrial stress along with the UPR^{mt}. Together, these two retrograde signalling branches act to alleviate stress through metabolic readjustments, promoting mitochondrial function and rescuing neurons.

Our data show that in *pink1* mutant flies, mitochondrial dysfunction results in the transcriptional upregulation of a subset of previously unidentified genes affecting key nucleotide metabolic processes, suggesting that these processes are needed for the response to Pink1 deficiency and to protect against its neurotoxic consequences. Although the nucleotide salvage pathway, which provides deoxyribonucleotides for the DNA precursors used in DNA repair or mtDNA replication, is well known to have a role in neuronal function, to our knowledge, its role in neurodegeneration has not been reported. We have shown that genetic and pharmacological manipulation of the nucleotide metabolism pathways reverses the phenotype of *pink1* mutant flies. Thus, we have identified the enhancement of nucleotide metabolism pathways as a potential strategy to improve mitochondrial function in flies and human cells.

We propose that the ability to modulate the mitochondrial function using dNs pools or FA might provide important avenues for neuroprotective therapy for PD and, more broadly, for other age-related neurodegenerative diseases associated with mitochondrial dysfunction. FA is a widely used dietary supplement in humans, and its safety is well established. The pharmacological manipulation of both the salvage and *de novo* pathways identified metabolites that were capable of suppressing the pathophysiological hallmarks of Pink1 dysfunction, raising the possibility of developing approaches for the protection against pathologies associated with mitochondrial dysfunction. Importantly, the concept of employing pharmacological approaches to suppress mitochondrial pathologies linked to Pink1 dysfunction was recently supported by a study showing that vitamin K_2 rescues mitochondrial impairment in *pink1* mutant flies[22].

Our data support the therapeutic potential of FA to enhance nucleotide pools, promoting mitochondrial biogenesis and improving mitochondrial function in neurons in neurodegenerative disease, and confirm a mechanism by which this acts. On the basis of our findings, we propose that a high-FA diet might be beneficial to modulate the pathogenesis of PD by repressing mitochondrial dysfunction, opening a promising avenue towards exploring the role of FA in the prevention of and therapy for neurodegenerative diseases such as PD. □

METHODS

Methods and any associated references are available in the online version of the paper.

Note: Supplementary Information is available in the online version of the paper

ACKNOWLEDGEMENTS

We would like to thank J. Silber (Institut Jacques Monod, France), A. Whitworth (University of Sheffield, UK), T. Rival (Aix-Marseille Université, France), the Vienna *Drosophila* RNAi Center and the Bloomington *Drosophila* Stock Center for fly stocks; and J. Parmar for fly food preparation. We thank D. Green for comments on the manuscript and helpful discussions. We thank A. Antonov for advice on advanced biostatistics. We also thank M. Locker for helpful discussions.

AUTHOR CONTRIBUTIONS

A.Y.A., G.R.M., L.M.M., R.T. and S.H.Y.L. conceived and designed the experiments. A.Y.A., D.D., I.P.d.C., L.M.M., P.R.A., R.T., S.G., S.L. and S.H.Y.L. performed the experiments and analysed the data. R.T. did most of the experimental work and analysis. E.D. contributed materials. A.E.W., H.P-F. and P.N. provided experimental and conceptual advice. G.R.M., L.M.M., R.T., S.G. and S.H.Y.L wrote the paper. S.H.Y.L. and L.M.M. contributed equally as joint last authors.

COMPETING FINANCIAL INTERESTS

The authors declare no competing financial interests.

Published online at www.nature.com/doifinder/10.1038/ncb2901
Reprints and permissions information is available online at www.nature.com/reprints

1. Deas, E., Plun-Favreau, H. & Wood, N. W. PINK1 function in health and disease. *EMBO Mol. Med.* **1,** 152–165 (2009).
2. Tatsuta, T. & Langer, T. Quality control of mitochondria: protection against neurodegeneration and ageing. *EMBO J.* **27,** 306–314 (2008).
3. Broadley, S. A. & Hartl, F. U. Mitochondrial stress signaling: a pathway unfolds. *Trends Cell Biol.* **18,** 1–4 (2008).
4. Lu, B. & Vogel, H. *Drosophila* models of neurodegenerative diseases. *Annu. Rev. Pathol.* **4,** 315–342 (2009).
5. Pimenta de Castro, I. *et al.* Genetic analysis of mitochondrial protein misfolding in *Drosophila melanogaster*. *Cell Death Differ.* **19,** 1308–1316 (2012).
6. Arner, E. S. & Eriksson, S. Mammalian deoxyribonucleoside kinases. *Pharmacol. Ther.* **67,** 155–186 (1995).
7. Curbo, S., Amiri, M., Foroogh, F., Johansson, M. & Karlsson, A. The *Drosophila melanogaster* UMP-CMP kinase cDNA encodes an N-terminal mitochondrial import signal. *Biochem. Biophys. Res. Commun.* **311,** 440–445 (2003).
8. Munch-Petersen, B., Piskur, J. & Sondergaard, L. Four deoxynucleoside kinase activities from *Drosophila melanogaster* are contained within a single monomeric enzyme, a new multifunctional deoxynucleoside kinase. *J. Biol. Chem.* **273,** 3926–3931 (1998).
9. Breitling, R., Armengaud, P., Amtmann, A. & Herzyk, P. Rank products: a simple, yet powerful, new method to detect differentially regulated genes in replicated microarray experiments. *FEBS Lett.* **573,** 83–92 (2004).
10. Breitling, R., Amtmann, A. & Herzyk, P. Iterative Group Analysis (iGA): a simple tool to enhance sensitivity and facilitate interpretation of microarray experiments. *BMC Bioinform.* **5,** 34 (2004).
11. Kikuchi, G., Motokawa, Y., Yoshida, T. & Hiraga, K. Glycine cleavage system: reaction mechanism, physiological significance, and hyperglycinemia. *Proc. Jpn. Acad. B* **84,** 246–263 (2008).
12. Hassel, B. Carboxylation and anaplerosis in neurons and glia. *Mol. Neurobiol.* **22,** 21–40 (2000).
13. Icreverzi, A., de la Cruz, A. F., Van Voorhies, W. A. & Edgar, B. A. *Drosophila* cyclin D/Cdk4 regulates mitochondrial biogenesis and aging and sensitizes animals to hypoxic stress. *Cell Cycle* **11,** 554–568 (2012).
14. Ziviani, E., Tao, R. N. & Whitworth, A. J. *Drosophila* parkin requires PINK1 for mitochondrial translocation and ubiquitinates mitofusin. *Proc. Natl Acad. Sci. USA* **107,** 5018–5023 (2010).
15. Morais, V. A. *et al.* Parkinson's disease mutations in PINK1 result in decreased Complex I activity and deficient synaptic function. *EMBO Mol. Med.* **1,** 99–111 (2009).
16. Park, J. *et al.* Mitochondrial dysfunction in *Drosophila* PINK1 mutants is complemented by parkin. *Nature* **441,** 1157–1161 (2006).
17. Wills, J. *et al.* Elevated tauopathy and alpha-synuclein pathology in postmortem Parkinson's disease brains with and without dementia. *Exp. Neurol.* **225,** 210–218 (2010).
18. Clark, I. E. *et al. Drosophila pink1* is required for mitochondrial function and interacts genetically with *parkin*. *Nature* **441,** 1162–1166 (2006).
19. Gandhi, S. *et al.* PINK1-associated Parkinson's disease is caused by neuronal vulnerability to calcium-induced cell death. *Mol Cell* **33,** 627–638 (2009).
20. Allen, J. F. Control of gene expression by redox potential and the requirement for chloroplast and mitochondrial genomes. *J. Theor. Biol.* **165,** 609–631 (1993).
21. Butow, R. A. & Avadhani, N. G. Mitochondrial signaling: the retrograde response. *Mol. Cell* **14,** 1–15 (2004).
22. Vos, M. *et al.* Vitamin K2 is a mitochondrial electron carrier that rescues pink1 deficiency. *Science* **336,** 1306–1310 (2012).

METHODS

Microarray acquisition and analysis. RNA was prepared from 3-day-old male adult flies (6 samples in total, 3 replicates for each genotype). The RNA quality was confirmed using an Agilent 2100 Bioanalyzer. The target samples were prepared following the GeneChip One-Cycle Target Labelling protocol (Affymetrix). All of the samples were then hybridized to GeneChip *Drosophila* Genome 2.0 arrays (Affymetrix). The arrays were washed and stained using Affymetrix protocols on a Fluidics Station 400, scanned using a Gene Array Scanner 2500 and deposited at ArrayExpress under accession number E-MEXP-3645. Differential expression was analysed by the UK *Drosophila* Affymetrix Array Facility (University of Glasgow) with RankProducts and iterative Group Analysis using the automated FunAlyse pipeline.

A network analysis was performed on the list of upregulated genes with a false discovery rate (FDR) below 50% using R-Spider, a web-based tool that integrates gene lists with the Reactome and KEGG databases[23].

RNA extraction and real-time PCR. Isolation of total RNA was performed using the RNeasy Mini Kit (QIAGEN). Quantitative real-time PCR with reverse transcription (qRT–PCR) was performed on an Mx4000 (Stratagene) real-time cycler using the QuantiTect SYBR Green RT–PCR system (QIAGEN). Gene-specific primers were obtained from QIAGEN (QuantiTect Primer Assays) for the following genes: CG3999 (catalogue number QT00972349), CG3011/Shmt2 (catalogue number QT00498904), CG6415 (catalogue number QT00934318), CG18466-RB/Nmdmc (catalogue number QT00503153), CG14887-RA/Dhfr (catalogue number QT00976227), CG11089/atic (catalogue number QT00982023), CG9127-RA/ade2 (catalogue number QT01084958), CG5452-RA/*dNK* (catalogue number QT0097774), *actin 79B* (catalogue number QT00967393). The relative transcript levels of each target gene were normalized against *actin* mRNA levels; quantification was performed using the comparative Ct method[24].

Metabolic profiling. Global metabolic profiles were obtained for each individual genotype using the Metabolon Platform (Metabolon). Briefly, each sample consisted of 8 biological replicates (100 flies per replicate). The sample preparation process was carried out using the automated MicroLab STAR system from Hamilton Company. For sample extraction, a 80% (v/v) methanol/water solution was used. Recovery standards were added before the first step in the extraction process for quality control purposes. Sample preparation was conducted using a proprietary series of organic and aqueous extractions to remove the protein fraction while allowing maximum recovery of small molecules. The resulting extract was divided into two fractions; one for analysis by LC and one for analysis by GC. Samples were placed briefly on a TurboVap (Zymark) to remove the organic solvent. Each sample was then frozen and dried under vacuum. Samples were then prepared for the appropriate instrument, either LC/MS or GC/MS. Compounds above the detection threshold were identified by comparison to library entries of purified standards or recurrent unknown entities. Identification of known chemical entities was based on comparison to metabolomic library entries of purified standards.

Gene network analysis. We used R-Spider[23] to construct a single connected network based on upregulated transcripts found in *pink1* mutant flies. We first submitted a list of 1,693 upregulated genes, selected with an FDR of 50%, to the R-Spider analysis through a dialogue-driven web interface[25]. From this list, we were able to connect 68 genes into a network of 92 nodes (Supplementary Fig. 1c and Table 3). We then reduced the FDR threshold to 5% to obtain a list of network components below this threshold.

Genetics and *Drosophila* strains. Fly stocks and crosses were maintained on standard cornmeal agar media at 25 °C. The strains used were UAS–*dNK* (ref. 26), *pink1*^{B9} (ref. 16), *park*^{25}, UAS–*pink1* and UAS–*parkin* (kind gifts from A. Whitworth, MRC, Centre for Developmental and Biomedical Genetics, University of Sheffield, Sheffield, UK), *da*–GAL4 and *elav*–GAL4 (Bloomington *Drosophila* Stock Center) and Tfam RNAi line (Transformant ID: 107191, Vienna *Drosophila* RNAi Center). The genotypes for all of the flies used in this study are listed in Supplementary Table 8. For crosses to combine *pink1*^{B9} mutants with GAL4/UAS transgenes, paternal males with a marked X chromosome (y- or FM6) were used to allow for the correct identification of *pink1*^{B9} mutant progeny. The deletion of the *pink1*-coding region (570 base pairs, as described in ref. 16) and the loss of *pink1* mRNA were routinely detected using PCR and qRT–PCR, respectively.

BrdU ELISA in *Drosophila* adult tissues. Assessment of mtDNA synthesis was performed using a BrdU enzyme-linked immunosorbent assay (ELISA). After 40 h of exposure to food containing 50 mM BrdU (SIGMA, catalogue number B5002), individual adult males were anaesthetized and immediately homogenized in 400 µl of chilled homogenization buffer (0.25 M sucrose, 10 mM EDTA and 30 mM Tris-HCl, at pH 7.5). After 10 min of incubation on ice, lysates were centrifuged at 2700 r.p.m. (700*g*) at 4 °C for 5 min. Supernatants were then transferred into fresh tubes and centrifuged at 10,400 r.p.m. (10,000*g*) at 4 °C for 30 min. The supernatants were discarded, and mitochondrial pellets were resuspended in 30 µl of 100 mM Tris-HCl, at pH 8.5, containing 5 mM EDTA, 0.2% (w/v) SDS, 200 mM NaCl and 100 µg ml^{-1} proteinase K. The samples were kept on ice for 10 min and incubated at 55 °C in a thermal mixer for 3 h. After centrifugation at maximum speed, the supernatants were recovered and 100 µl of absolute ethanol was added. The samples were mixed and kept at −20 °C for at least 10 min (up to 16 h).

After centrifugation at maximum speed, the resulting mitochondrial pellets were dried and resuspended in PBS containing 0.1% BSA. Following denaturation at 98 °C for 30 min, samples were immediately placed at 4 °C and loaded (100 µl per well) onto a 96-well microtitre plate (MaxiSorb, Nunc). The BrdU ELISA was performed according to ref. 27.

Quantification of mtDNA. Analysis of the mtDNA content was performed by qPCR as previously described[28].

ATP assays. Five thoraces (or whole flies, or eleven heads, depending on the experiment) from 2-day-old flies were dissected and processed as previously described[29].

Respirometry analysis. Mitochondrial respiration was assayed at 37° C by high-resolution respirometry as previously described[29].

Behavioural analysis. For the climbing assay, 10 male flies at the indicated age were placed into glass columns (23 cm long, 2.5 cm in diameter) that were lined with nylon mesh (250 micrometres, Dutscher Scientific) and marked with a line at 15 cm. After a 30–60 min recovery from CO_2 anaesthesia, flies were gently tapped to the bottom of the vial, and the time required for 5 flies to climb above the marked line was recorded. For each experiment, at least three cohorts of 10 flies from each genotype were scored, and all of the experiments were performed in triplicate. For the locomotor assay, male flies were individually placed in *Drosophila* Activity Monitoring System (DAMS; TriKinetics) testing chambers (capped with standard cornmeal agar media at one end). The flies were grown in a light/dark 12 h:12 h cycle at 25 °C. Data were exported into Excel, and the average total locomotor activity (as measured by the total number of recorded midline crossings per hour) was calculated for each genotype ($n = 16$ per genotype). All of the experiments were performed in triplicate. Flight assays were performed as previously described[22]. These flight assays are likely to have different sensitivities when compared with other approaches[16,30].

Data acquired for the assessment of both genetic and pharmacological rescue of either *pink1* or *parkin* mutants were obtained as a single experimental set before statistical analysis.

Longevity assays. Groups of 10 newly eclosed males of each genotype were placed into separate vials with food and maintained at 25 °C. Flies were transferred into vials containing fresh food every 2–3 days, and the number of dead flies was recorded. Data are presented as Kaplan–Meier survival distributions, and the significance was determined by log-rank tests.

Electron microscopy. This was performed as previously described[28].

Antibodies. Primary antibodies employed in this study were oxidative phosphorylation rodent cocktail, and NDUFS3/complex I 1:1,000 (Mitosciences), mtTFA (TFAM) 1:1,000 (Abcam, ab47548), tyrosine hydroxylase 1:1,000 (Millipore), α-tubulin 1:5,000 (SIGMA), SOD1 1:1,000 (SOD-100, Stressgen), SOD2 1:1,000 (SOD-110, Stressgen), dMfn 1:1,000 (a kind gift from A. Whitworth, MRC, Centre for Developmental and Biomedical Genetics, University of Sheffield).

Protein extraction and western blotting. Protein extracts from whole flies or heads were prepared by grinding flies in lysis buffer (25 mM Tris-HCl at pH 7.4, 300 mM NaCl, 5 mM EDTA, 1 mM phenylmethylsulphonyl fluoride and 0.5% (w/v) Nonidet-40) containing the protease inhibitors leupeptin, antipain, chymostatin and pepstatin (SIGMA) at the manufacturer's recommended dilution. The suspensions were cleared by centrifugation at 15,700*g* for 10 min at 4 °C and protein concentrations of the supernatants were estimated using the Bradford assay (Bio-Rad). After adding 10% (w/v) SDS, aliquots of each fraction were mixed with 2 X SDS loading buffer. For SDS–PAGE, equivalent amounts of proteins were resolved on 10% Precast Gels (Invitrogen) and transferred onto nitrocellulose membranes. The membranes were blocked in TBS (0.15 M NaCl and 10 mM Tris-HCl; pH

DOI: 10.1038/ncb2901

7.5) containing 5% (w/v) dried non-fat milk (blocking solution) for 1 h at room temperature, probed with the indicated primary antibody before being incubated with the appropriate HRP-conjugated secondary antibody. Antibody complexes were visualized by Pierce enhanced chemiluminescence (ECL).

Microscopy-based assessment of mitochondrial function and density. For measurements of $\Delta\psi m$ in fly brains, these were loaded for 40 min at room temperature with 40 nM tetramethylrhodamine methylester (TMRM) in loading buffer (10 mM HEPES at pH 7.35, 156 mM NaCl, 3 mM KCl, 2 mM $MgSO_4$, 1.25 mM KH_2PO_4, 2 mM $CaCl_2$ and 10 mM glucose) and the dye was present during the experiment. In these experiments, TMRM is used in the redistribution mode to assess $\Delta\psi m$, and therefore a reduction in TMRM fluorescence represents mitochondrial depolarization. Confocal images were obtained using a Zeiss 710 CLSM equipped with a ×40 oil immersion objective. Illumination intensity was kept to a minimum (at 0.1–0.2% of laser output) to avoid phototoxicity and the pinhole was set to give an optical slice of 2 µm. Fluorescence was quantified in individual mitochondria by exciting TMRM using the 565 nm laser and fluorescence was measured above 580 nm. *Z*-stacks of 4–5 fields per brain were acquired, and the mean maximal fluorescence intensity was measured for each group. The differences in $\Delta\psi m$ are expressed as a percentage compared with control brains (taken as 100%). Mitochondrial mass was calculated as the percentage of co-localization of the TMRM fluorescence (mitochondria) and calcein blue (whole neurons). Brains were loaded with 40 nM TMRM and 5 µM calcein blue AM for 40 min at room temperature in loading buffer. Calcein blue was excited using the 405 nm laser and fluorescence was measured above 430 nm. Data acquired for the assessment of both genetic and pharmacological rescue of either *pink1* or *parkin* mutants were obtained as a single experimental set before statistical analysis.

For measurements of $\Delta\psi m$ in human neuroblastoma cells, these were loaded with 25 nM TMRM for 30 min at room temperature, and the dye was present during the experiment. TMRM is used in the redistribution mode to assess $\Delta\psi m$ in individual mitochondria, and therefore a reduction in TMRM fluorescence represents mitochondrial depolarization. NADH autofluorescence was excited at 351 and measured at 375–470 nm.

Analysis of dopaminergic neurons. Fly brains were dissected from 20-day-old flies and stained for anti-tyrosine hydroxylase (Immunostar) as described previously[31]. Brains were mounted on Vectashield (Vector Laboratories), imaged by confocal microscopy and tyrosine hydroxylase-positive PPL1 cluster neurons were counted per brain hemisphere. Data acquired for the assessment of both genetic and pharmacological rescue of either *pink1* or *parkin* mutants were obtained as a single experimental set before statistical analysis.

Oxidative stress assay. The procedure used for longevity assay was repeated for oxidative stress assays using food containing paraquat or antimycin at the indicated concentration. Data are presented as Kaplan–Meier survival distributions and significance was determined by log-rank tests.

Analysis of post-mortem human samples. Flash-frozen post-mortem brain tissue was obtained from the Queen Square Brain Bank (QSBB) after acquiring ethical approval from the National Hospital of Neurology and Neurosurgery (NHNN), the Local Research Ethics Committee (LREC) and the Research and Development department of University College Hospital London (UCLH). Informed consent had been acquired by the QSBB. All of the tissue had Caucasian ancestry. Three flash-frozen post-mortem brains with classical neuropathological appearances of Parkinson's disease, associated with heterozygous mutations in the *PINK1* gene, were originally identified in an extensive mutation screen[32]. Four flash-frozen control brains were used as age-matched and pH-matched controls. A total of 70–90 mg of tissue was homogenized and RNA was extracted using an RNeasy mini kit (Qiagen) according to the manufacturer's protocol. Briefly, 1 ml of Qiazol was added to a 90 mg sample, and the mixture was homogenized using a Qiagen TissueRuptor with disposable probes for cell lysis. After homogenization, 200 µl chloroform was added and the mixture was mixed. The subsequent aqueous and organic layers were separated by centrifugation at 10,000*g* for 30 min at 4 °C. The upper aqueous phase containing the RNA was removed and 200 µl of 70% glacial ethanol was added. The mixture was applied to the silica gel matrix and centrifuged at 8,000*g* for 15 s to allow RNA to be absorbed onto the membrane. Contaminants were washed through (8,000*g* for 15 s). RNA was then eluted in >50 µl RNase-free H_2O and stored at −80 °C. All RNA preparations were analysed on a Nanodrop ND-1000 spectrophotometer (Thermo Scientific) to determine the RNA concentration and yield, and on an Agilent 2100 Bioanalyzer (Agilent Technologies) using the Eukaryote Total RNA Nano Assay to determine the quality of the RNA using the RNA integrity number (RIN). The latter is a software algorithm developed by Agilent Technologies to standardize assessment of RNA quality. The algorithm is based on a number of features that denote RNA integrity, including the ratio of the two main species of ribosomal RNA (18S and 28S) and the relative height of the 28S rRNA peak. RIN of 0 indicates completely degraded or undetectable RNA and RIN of 10 indicates intact RNA with no degradation[33].

qRT–PCR was performed on an Mx4,000 (Stratagene) real-time cycler using the QuantiTect SYBR Green RT–PCR system (QIAGEN). Gene-specific primers were obtained from QIAGEN (QuantiTect Primer Assays) for the following genes: Hs_DHFR (catalogue number QT01668730), Hs_ATIC (catalogue number QT00015526), Hs_PAICS (catalogue number QT00087458), Hs_TK2 (catalogue number QT00071428). GADPH primers were from SIGMA (forward primer: 5′-GAAGGTGAAGGTCGGAGT-3′; reverse primer: 5′-GAAGATGGTGATGGGATTTC-3′). The Ct value of each target gene was normalized by the subtraction of the Ct value from the housekeeping gene—*GADPH*—to obtain the ΔCt value. The relative gene expression level was shown as ΔCt, which is inversely correlated to the gene expression level.

Statistical analysis. Descriptive and inferential statistics analyses were performed using GraphPad Prism 5 (www.graphpad.com). Computation of the minimal sample size for the variables measured in this study was assessed by power analysis, setting alpha initially to 0.05, employing StatMate 2 (www.graphpad.com).

Data are presented as the mean values, and the error bars indicate ±s.d. or ±s.e.m., as indicated. The number of biological replicates per experimental variable (n) is indicated in the figure legends. Parametric tests were used, after confirming that the variables under analysis exhibited Gaussian distributions, using the D'Agostino–Pearson test (performed using data obtained from pilot experiments and computed using GraphPad Prism 5). The significance is indicated as *** for $P < 0.001$, ** for $P < 0.01$, * for $P < 0.05$. For the statistical analysis of biochemicals in flies, pair-wise comparisons were performed using Welch's t-tests. The q-value provides an estimate of the FDR according to ref. 34. The investigators gathering quantitative data on biological samples were blinded to the sample identities at the time of analysis. No specific randomization strategies were employed when assigning biological replicates to treatment groups.

Digital image processing. Fluorescence, transmission electron microscope and western blot images were acquired as uncompressed bitmapped digital data (TIFF format) and processed using Adobe Photoshop CS3 Extended, employing established scientific imaging workflows[35]. Images shown are representative of at least three independent experiments.

23. Antonov, A. V., Schmidt, E. E., Dietmann, S., Krestyaninova, M. & Hermjakob, H. R spider: a network-based analysis of gene lists by combining signaling and metabolic pathways from Reactome and KEGG databases. *Nucleic Acids Res.* **38,** W78–W83 (2010).
24. Schmittgen, T. D. & Livak, K. J. Analyzing real-time PCR data by the comparative C(T) method. *Nat. Protoc.* **3,** 1101–1108 (2008).
25. Antonov, A. V. BioProfiling.de: analytical web portal for high-throughput cell biology. *Nucleic Acids Res.* **39,** W323–W327 (2011).
26. Legent, K. *et al.* *In vivo* analysis of *Drosophila* deoxyribonucleoside kinase function in cell cycle, cell survival and anti-cancer drugs resistance. *Cell Cycle* **5,** 740–749 (2006).
27. Behl, B. *et al.* An ELISA-based method for the quantification of incorporated BrdU as a measure of cell proliferation *in vivo*. *J. Neurosci. Methods* **158,** 37–49 (2006).
28. De Castro, I. P. *et al.* *Drosophila* ref(2)P is required for the parkin-mediated suppression of mitochondrial dysfunction in pink1 mutants. *Cell Death Dis.* **4,** e873 (2013).
29. Costa, A. C., Loh, S. H. & Martins, L. M. *Drosophila* Trap1 protects against mitochondrial dysfunction in a PINK1/parkin model of Parkinson's disease. *Cell Death Dis.* **4,** e467 (2013).
30. Poole, A. C. *et al.* The PINK1/Parkin pathway regulates mitochondrial morphology. *Proc. Natl Acad. Sci. USA* **105,** 1638–1643 (2008).
31. Whitworth, A. J. *et al.* Increased glutathione S-transferase activity rescues dopaminergic neuron loss in a *Drosophila* model of Parkinson's disease. *Proc. Natl Acad. Sci. USA* **102,** 8024–8029 (2005).
32. Abou-Sleiman, P. M. *et al.* A heterozygous effect for PINK1 mutations in Parkinson's disease? *Ann. Neurol.* **60,** 414–419 (2006).
33. Schroeder, A. *et al.* The RIN: an RNA integrity number for assigning integrity values to RNA measurements. *BMC Mol. Biol.* **7,** 3 (2006).
34. Storey, J. D. & Tibshirani, R. Statistical significance for genomewide studies. *Proc. Natl Acad. Sci. USA* **100,** 9440–9445 (2003).
35. Wexler, E. J. Photoshop CS3 Extended: Research Methods and Workflows, lynda.com (2008).